Uncertainty and Sensibility Analysis of Loss of Forced Cooling Accident of a 150MWt Molten Salt Reactor*

Kai Wang,[1,2] Chaoqun Wang,[1,2] Qun Yang,[1,2] Zhaozhong He,[1] and Naxiu Wang[1,†]

[1]*Shanghai Institute of Applied Physics, Chinese Academy of Sciences, 201800 Shanghai, China*
[2]*University of Chinese Academy of Sciences, 100049 Beijing, China*

Molten salt reactors (MSRs) have been selected as one of the promising candidate Generation IV reactor technologies, and the small modular molten salt reactor (SM-MSR), which utilizes low-enriched uranium and thorium fuels, is regarded as a wise development path to speed deployment time. Uncertainty and sensibility analysis of accidents possess a great guidance in nuclear reactor design and safety analysis. Uncertainty analysis can ascertain the safety margin, and sensitivity analysis can reveal the correlation between accident consequences and input parameters. Loss of forced cooling (LOFC) represents an accident scenario of SM-MSR, and the study of LOFC could offer useful information to improve physics thermohydraulic and structure designs. Therefore, the uncertainty of LOFC consequences and the sensibility of related parameters were focused on in this paper. The uncertainty of LOFC consequences was analyzed by performing Monte-Carlo method and the multiple linear regression method was employed to analyze the sensibility of input parameters. The uncertainty and sensibility analysis show that the maximum reactor outlet fuel salt temperature was $725.5\,^{\circ}\mathrm{C}$ which is lower than the acceptable criterion, and 5 important parameters influencing LOFC consequences were pinpointed.

Keywords: molten salt reactor, LOFC, uncertainty analysis, sensibility analysis

I. INTRODUCTION

Molten salt reactors (MSRs) have been selected as one of the promising candidate Generation IV reactor technologies[1–3], due to the advantages of inherent safety[4–9] and high economic efficiency[10–14]. In 2011, the Chinese Academy of Sciences (CAS) started the Strategic Priority Research Program named the Future Advanced Nuclear Fission Energy, and the molten salt reactor was one of the project options. And then a small modular molten salt reactor (SM-MSR) was proposed[15]. Safety analysis plays a key role in molten salt reactor design. It is performed to ensure that the reactor design meets the relevant safety requirements set by the operating organization and the regulators, and also applied in optimizing design and improving safety performance. One important event in safety analysis is the loss of forced cooling (LOFC) accident which is of great significant to ensure the design adheres to prescribed and acceptable limits for radiation doses and releases under various plant conditions.

The use of best estimate codes, along with uncertainties evaluation so-called BEPU methodologies[16] is an accepted procedure by the regulatory authorities for conducting deterministic safety analysis. At the end of the 1980's, the US Nuclear Regulatory Commission decided to permit the use of best estimate methods with uncertainty quantification for reactor safety analysis, in lieu of the earlier licensing practice that used deterministic methods with conservative assumptions to address uncertainties[17]. The BEPU approach calculates the uncertainty associated with the value provided by a best-estimate code to realistically estimate the safety margin of the safety criteria. Through combination with sensitivity studies, the significance of input parameters can be identified and quantified.

Some researchers have been engaged in the uncertainty and sensibility analysis of molten salt reactors. X.W. Jiao et al.[18] adopted RELAP5/ MOD4.0 to study the significance of the trip setpoint in a reactivity-initiated accident and given the sensitivity rankings of the trip setpoint parameters. X.W. Jiao et al.[19] also studied the sensitivity of initial conditions during a reactivity-initiated accident under low power conditions of a molten salt reactor and the results show that the consequences of reactivity introduced events have low sensitivity to the temperature coefficients of reactivity. M. Santanoceto et al.[20] studied the uncertainty and sensitivity of the molten salt fast reactor steady-state using a polynomial chaos expansion method and the analysis performed on the whole temperature field shows that the heat exchanger can be a critical component. J.J. Wang et al.[21] studied the uncertainty of heat transfer of TMSR-SF0 simulator and the simulation results indicate that the uncertainty propagated to core outlet temperature is about $\pm 10\,^{\circ}\mathrm{C}$ with a confidence interval of 95% for a steady-state operation condition. While previous studies have explored uncertainty and sensitivity analysis in molten salt reactors, most of them concentrated on steady-state or specific parameters, and the comprehensive uncertainty and sensibility study of accident was insufficient so far. In this study, the comprehensive uncertainty of LOFC consequences and the sensibility of related input parameters were focused on.

II. DESCRIPTION OF SM-MSR

Fig. 1 illustrates the schematic design of the SM-MSR, and the main design parameters are listed in Table 1. The reactor adopts a double molten salt circuit design. The primary circuit components include a reactor core, intermediate heat exchangers (IHX), control rods, a primary pump,

* Supported by the Youth Innovation Promotion Association (YIPA) (Grant No. E329290101) of the Chinese Academy of Sciences.

† Corresponding author, Naxiu Wang, wangnaxiu@sinap.ac.cn.

and pipelines. The reactor core consists of open-celled graphite elements forming 241 molten salt channels and 6 functional channels for control rods. The fuel salt is made of $\mathrm{LiF-BeF_2-ZrF_4-UF_4-ThF_4}$, it enters the reactor at approximately 629 °C through the lower plenum, ascends through the reactor core where nuclear fission reactions occur and the fuel salt is heated, and it finally exits the reactor core at approximately 700 °C[15].

The secondary circuit consists of a secondary pump, molten-salt-air heat exchangers (AHX) and pipelines. The coolant salt of the secondary circuit is made of $\mathrm{LiF-NaF-KF}$, and it is pumped into the tube side of the primary heat exchanger to remove the primary circuit power, and then discharging the heat to the Brayton cycle system through the molten-salt-air heat exchanger. Finally, the nuclear power is converted into electrical energy through the Brayton cycle turbine.

To mitigate the accident consequences, a natural circulation flow loop is implemented for decay heat removal, formed between the hot core and heat exchangers (PHX) of the pool reactor auxiliary cooling system (PRACS). During normal operation condition, the PRACS flow path is partially blocked by a check valve, which has much larger loss coefficients for reversed flow compared to forward flows. The PHX modules transfer heat from the primary salt to the buffer salt, and then the buffer salt is cooled by direct reactor auxiliary cooling system (DRACS) modules, the DRACS transfer heat through natural circulation flow from the buffer salt to a molten salt-air heat exchangers (ADHX), and finally cooled by outside ambient air. Notably, all the components in contact with molten salt are constructed from Hastelloy-N.

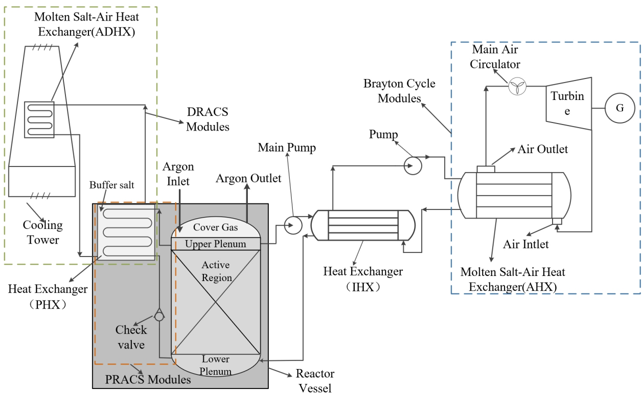

Fig. 1. Schematic of the 150MWt molten salt reactor.

III. METHODOLOGY

Currently, there are two general approaches for uncertainty analysis: the propagation of input uncertainty and extrapolation of output accuracy[22, 23]. Extrapolation of output accuracy requires lots of experimental data. Considering the limited number of current molten salt reactor experiments, this study adopts the propagation of input uncertainty approach, which is based on Monte Carlo methods. The propagation of input uncertainty approach is based on two elements: association of uncertainty to input parameters and multiple executions of the best-estimate code. A flowchart for performing the SM-MSR LOFC accident uncertainty and sensitivity analysis is illustrated in Fig. 2.

Table 1. Main parameters of the 150MWt molten salt reactor design.

Main Parameter	Design Value
Thermal power	150MWt
Fuel salt composition	$\mathrm{LiF-BeF_2-ZrF_4-UF_4-ThF_4}$
Fuel salt temperature(inlet\outlet)	629 °C\700 °C
Diameter × height of reactor body	3.54 m × 3.6 m
Fuel salt power density	$66\ \mathrm{MW/m^3}$
Lifetime of reactor body	10 years
Graphite structure	Hexagonal prism
The secondary circuit salt composition	$\mathrm{LiF-NaF-KF}$
PRACS salt composition	$\mathrm{LiF-BeF_2-ZrF_4-UF_4-ThF_4}$
DRACS salt composition	$\mathrm{LiF-NaF-KF}$
Design power of PRACS and DRACS	2%FP
Structure material	Hastelloy-N

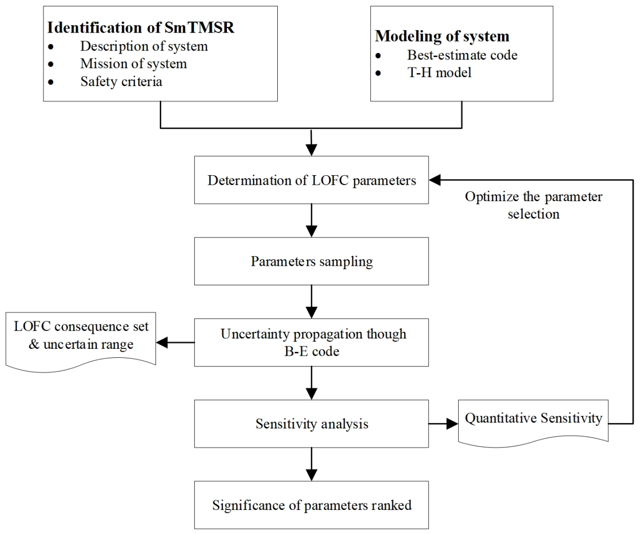

Fig. 2. Procedures of uncertainty and sensitivity analysis of the SM-MSR.

A. Uncertainty Parameters

The uncertainty of input parameters stems from the imprecise knowledge of the actual value, with sources of uncertainty consist of reactor system data, structural material properties, and B-E code correlations. Uncertain parameters for the LOFC accident were selected by the phenomena identification and ranking table (PIRT). The primary approach for quantifying input uncertainty includes both probabilistic and deterministic methods. Probabilistic methodologies utilize statistical elements to characterize and combine input uncertainty, while deterministic methodologies use rea-

sonable ranges or bounding intervals of uncertainty and combine the input uncertainty based on maximization and minimization of the output value[24–26]. The probabilistic approach is the most widely adopted procedure and is endorsed by industry and regulators currently. The limited detailed information about certain aspects of SM-MSR is a significant drawback. To minimize the impact of this drawback, a list of input parameters along with their associated density functions is adopted by using a probabilistic methodology. As for the quantification of uncertainty parameters, it is established through previous studies, experimental data and expert judgment. In this study, 30 uncertainty input parameters were indentified, and Table 2 shows these parameters and their probability distribution functions used in this study.

B. Best-Estimate Code

The RELAP5 code is a transient analysis code designed for light water reactors, developed by the U.S. Nuclear Regulatory Commission (NRC) for various applications such as rule-making, licensing audit calculations, and evaluation of operator guideline. It uses one-dimensional and two-fluid thermal hydraulics model. The latest version RELAP5/MOD4.0 was developed by Innovative System Software (ISS) specifically for the analysis of nuclear power plants[27].

In RELAP5/MOD4.0, an uncertainty analysis package has been incorporated, following the methodology developed by Gesellschaft für Anlagenund Reaktorsicherheit (GRS)[24]. This methodology integrates order statistics and Wilks' formula[28, 29] into the propagation of input uncertainty approach. Since heat transfer coefficient correlations and coolants for the SM-MSR are not available in the current RELAP5/MOD4.0, new correlations[30] and coolants applied to MSRs have been inserted, and the updated code named RELAP5-TMSR[31–33]. In consideration of that the uncertainty analysis package can only be employed for partial analysis of light water reactors, an uncertainty analysis package for molten salt reactors systems was developed during this study. It can propagate uncertainties associated with the molten salt properties and uncertainties related to the inserted heat transfer correlations which are applicable for fuel channel in the reactor core and heater exchangers of SM-MSR.

C. Sensitivity Analysis method

Sensitivity analysis assesses the impact of varying values of independent variables on a particular dependent variable within defined assumptions. In other words, it studies how uncertainties in a mathematical model from various sources contribute to the overall model uncertainty.

Linear regression[34–36] utilizes a straight line to describe the relationship between variables. It identifies the best-fit line in a dataset by searching for the regression coefficient(s) value that minimizes the total error of the model. The model's equation presents clear coefficients that clarify the influence of each independent variable on the dependent variable. There are two primary types of linear regression:

1) Simple Linear Regression, which is the simplest form of linear regression, and it involves only one independent variable and one dependent variable.

2) Multiple Linear Regression (MLR), which involves more than one independent variable and one dependent variable. In this study, multiple linear regression (MLR) method is adopted. The equation for the multiple linear regression is shown in Eq. (1), where y is the dependent variable, x_i is independent variable, β_0 is the constant, β_i is coefficient.

$$y = \beta_0 + \beta_1\, x_1 + \beta_2\, x_2 + \ldots \beta_i\, x_i + \ldots + \beta_n\, x_n \qquad (1)$$

A systematic sensitivity analysis process based on MLR is shown in Fig. 3, which is proposed by G. Manache[37] and also applied in the functional reliability analysis of a molten salt natural circulation system[38]. The adjusted coefficient of determination (R^2_{adj}) is used to estimate whether the linear model is acceptable ($R^2_{adj} \geq 0.7$ means model is acceptable). The collinearity problem in the multiple linear regression is addressed by calculating the variance inflation factor (VIF) for each parameter, and VIF≤ 5 means weak collinearity. If the linear model is strongly collinear, a significance test of the semi-partial correlation coefficient (SPC) is used for the ranking of input uncertainty parameters, otherwise, the standardized regression coefficient (SRC) will be used for the significance test[38].

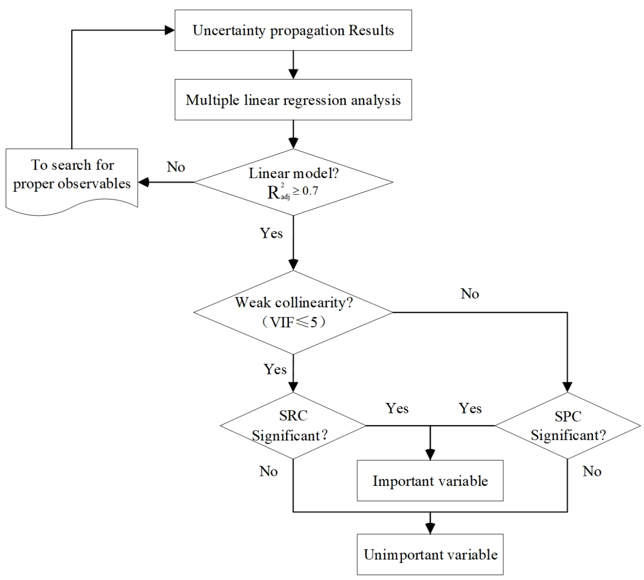

Fig. 3. Sensitivity analysis steps.

Table 2. Input uncertainty parameters of the SM-MSR.

No.	Parameters		Distribution	Range
p-1	Heat transfer coefficient of tube side	h_tube	Uniform	75%∼125%
p-2	Heat transfer coefficient of shell side	h_shell	Uniform	75%∼125%
p-3	Heat transfer coefficient of air side	h_air	Uniform	75%∼125%
p-4	Viscosity of fuel salt	ν_fuel	Uniform	90%∼110%
p-5	Heat conductivity of fuel salt	k_fuel	Uniform	90%∼110%
p-6	Coefficient of thermal expansion of fuel salt	b_fuel	Uniform	90%∼110%
p-7	Volumetric heat capacity of fuel salt	Cpv_fuel	Uniform	90%∼110%
p-8	Isothermal compressibility of fuel salt	e_fuel	Uniform	90%∼110%
p-9	Viscosity of FLiNaK	ν_flinak	Uniform	90%∼110%
p-10	Heat conductivity of FLiNaK	k_flinak	Uniform	90%∼110%
p-11	Coefficient of thermal expansion of FLiNaK	b_flinak	Uniform	90%∼110%
p-12	Volumetric heat capacity of FLiNaK	Cpv_flinak	Uniform	90%∼110%
p-13	Isothermal compressibility of FLiNaK	e_flinak	Uniform	90%∼110%
p-14	Thermal conductivity of graphite	k_graphite	Normal	90%∼110%
p-15	Volumetric heat capacity of graphite	cpv_graphite	Normal	90%∼110%
p-16	Thermal conductivity of Hastelloy-N	k_hn	Normal	90%∼110%
p-17	Volumetric heat capacity of Hastelloy-N	cpv_hn	Normal	90%∼110%
p-18	Reactor power	P_reactor	Uniform	95%∼105%
p-19	Control rod dropping time	t_drop	Uniform	80%∼120%
p-20	Reactor shutdown margin	ρ_shutdown	Uniform	80%∼120%
p-21	Fuel salt temperature coefficient of reactivity	ρ_f	Uniform	80%∼120%
p-22	Graphite temperature coefficient of reactivity	ρ_g	Uniform	80%∼120%
p-23	Core Hot Spot Factor	f_hsf	Uniform	80%∼120%
p-24	Atmospheric temperature	T_atmo	Uniform	95%∼105%
p-25	Local resistance coefficient of reactor core	f_core	Uniform	80%∼120%
p-26	Local resistance coefficient of primary circuit (excluding reactor core)	f_primary	Uniform	80%∼120%
p-27	Local resistance coefficient of PRACS	f_PRACS	Uniform	80%∼120%
p-28	Local resistance coefficient of 2nd circuit	f_second	Uniform	80%∼120%
p-29	Local resistance coefficient of DRACS	f_DRACS	Uniform	80%∼120%
p-30	Local resistance coefficient of air cooling tower	f_Airtower	Uniform	80%∼120%

IV. ANALYSIS AND RESULTS

A. Thermal-Hydraulic Model

Fig. 4 shows an overview of the RELAP5-TMSR nodalization of the SM-MSR. The whole system consists of four coupled parts:

1) The primary circuit, including downcomer, reactor core, lower plenum, upper plenum, primary pump, pipes and IHX tube side.

2) 2nd circuit, including pipes, 2nd circuit pump, IHX shell side and AHX tube side.

3) Brayton cycle modules, including air inlet volume, AHX shell side and air outlet volume.

4) Passive residual heat removal system which is consist of DRACS and PRACS, including pipes, PHX, ADHX and air cooling loop.

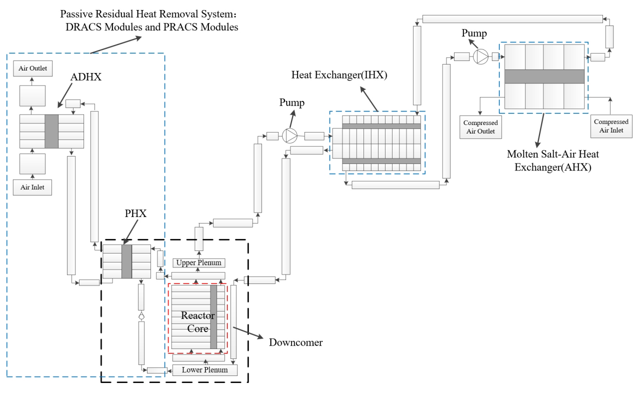

Fig. 4. Nodalization of the 150MWt molten salt reactor(MS-MSR).

B. Uncertainties and Sampling

Wilks' formula has been frequently used to quantify the minimum amount of computational work required to meaningfully assess a model's uncertainty by specifying acceptable tolerance limits on the model output parameter[39]. A fundamental advantage of using Wilks' formula is that it has no limit on the number of uncertainty parameters considered in the analysis. The number of code runs required in the uncertainty analysis only depends on the statistical features of the tolerance limits imposed, including percentile tolerance interval, confidence interval and order, and is irrelevant to the amount of the uncertain parameters[28, 29]. The number of code runs for the one-sided tolerance interval can be calcu-

lated by Eq. (2), where γ is the percentile tolerance interval, β is the confidence interval, N is the number of input samples(or number of code runs), m is the order.

$$\beta = 1 - \sum_{i=N-m+1}^{N} \frac{N!}{i!(N-i)!}\gamma^i (1-\gamma)^{N-i} \tag{2}$$

Table 3 shows the number of code runs based on Wilks' formula, varying with percentile tolerance and confidence intervals at different orders. In this study, the upper tolerance limit's percentile and confidence were set to the standard 95%/95% at the 5th order, and the minimum number of code runs is 181 by Wilks' formula.

Fig. 5 shows the cobweb plot of the 181 random samples for the 30 parameters, where the x-axis shows uncertain parameters and the y-axis shows normalized samples values. According to Fig. 5 the sample population achieved is well representative and meets the requirement of the LOFC uncertainty study.

Table 3. The number of code runs as a function of the percentile tolerance and confidence at different order by Wilks' formula.

Order	Confidence interval and percentile tolerance			
	0.90&0.90	0.95&0.95	0.97&0.97	0.99 &0.99
1st	22	59	116	459
2nd	38	93	177	662
3rd	52	124	231	838
4th	65	153	281	1001
5th	78	181	330	1157

C. Safety Variables and Acceptance criteria

The safety variables and their acceptance criteria are crucial in the safety analysis of SM-MSR. The primary circuit boundary serves as the principal safety barrier against radioactive leaks, so the performance of Hastelloy-N, which is used as the structural material for the primary circuit, is crucial to the reactor safety.

Temperature is a pivotal indicator of Hastelloy-N's performance, and some studies confirm its ability to maintain mechanical properties at 800 °C[40]. Meanwhile considering the direct contact of fuel salt with Hastelloy-N structural materials, the reactor outlet fuel temperature ($\mathrm{T_{out}}$) with a limiting value of 800 °C was selected as the criterion in this study.

D. Uncertainty propagation result

Once the code run numbers and sets of uncertain input parameters were established, input uncertainty was propagated through the RELAP5-TMSR code. During normal operating conditions, the flow in the core flow is driven by the pump at approximately 1000 kg/s. However, following an LOFC event, the pump stops, resulting in a decrease in core flow, which in turn causes an increase in $\mathrm{T_{out}}$ increase. At the same time, reactor protection system sends a shutdown signal, the control rods will drop, and then the power coasts down, and that will cause $\mathrm{T_{out}}$ decrease.

Under the influence of changes in core flow and nuclear power, $\mathrm{T_{out}}$ will reach its first peak at about 10s, reach the second peak at about 200s, and the second peak is the maximum point, since then $\mathrm{T_{out}}$ will change slowly, and finally will reach a safe and stable temperature, where decay heat continues to be removed by PRACS and DRACS.

The evolution of the $\mathrm{T_{out}}$ for the 181 code runs are shown in Fig. 6, and Fig. 7 shows the maximum value of reactor outlet fuel salt temperature ($\mathrm{T_{out\_max}}$) for the 181 cases, all results are lower than the acceptable criterion (800 °C), and the maximum value of $\mathrm{T_{out\_max}}$ is 725.5 °C, the minimum value of $\mathrm{T_{out\_max}}$ is 715.4 °C. Fig. 8 shows the upper and lower uncertainty bands, the maximum difference value between the upper and lower bounds is 18.5 °C during the initial temperature ascent phase. In the base case, the maximum temperature increase of reactor outlet fuel salt ($\Delta\mathrm{T_{out}}$) is 22.2 °C compared to the initial condition. In the upper limited case, $\Delta\mathrm{T_{out}}$ is 25.5 °C, representing a 26.2% increase relative to the base case, and as for the lower limited case, $\Delta\mathrm{T_{out}}$ is 15.4 °C, indicating a 23.7% decrease relative to base case.

E. Identification of $\mathrm{T_{out\_max}}$ Distribution

Fig. 9 shows the histogram and probability density function obtained from 181 simulations for $\mathrm{T_{out\_max}}$. The points roughly follow a bell curve shape in the histogram, indicating a normal distribution. In this study, the Shapiro-Wilk (S-W) test[41] is adopted to assess whether the calculated $\mathrm{T_{out\_max}}$ follows a normal distribution. The S-W test compares the observed dataset to the expected normal distribution to determine if the data set is normally distributed or not. The test statistic of the S–W test for normality is shown in Eq. 3, where $\mathrm{x_i}$ represents the ordered random sample values, $\bar{\mathrm{x}}$ is the mean of samples, and $\mathrm{a_i}$ the represents constants which is functions of n.

$$w = \frac{\left(\sum_{i=1}^{n} a_i x_i\right)^2}{\sum_{i=1}^{n} (x_i - \bar{x})^2} \tag{3}$$

The null hypothesis for the Shapiro-Wilk test is that the variable is normally distributed. If p<0.05, reject the null hypothesis, otherwise accept the null hypothesis. By statistical analysis, the obtained p-value is 0.197, which exceeds 0.05, so the null hypothesis of the normality is acceptable.

The quantile-quantile (Q-Q) plot is a graphical technique for determining whether two datasets come from populations with a common distribution[42]. In a Q-Q plot, if the data is normally distributed, the points will align on a straight diagonal line. Conversely, the more the points in the plot deviate significantly from this line, the less likely the dataset follows a normal distribution. Fig. 10 shows Q-Q plot for $\mathrm{T_{out\_max}}$, where points mostly lie along the straight diagonal line with some minor deviations along the tail.

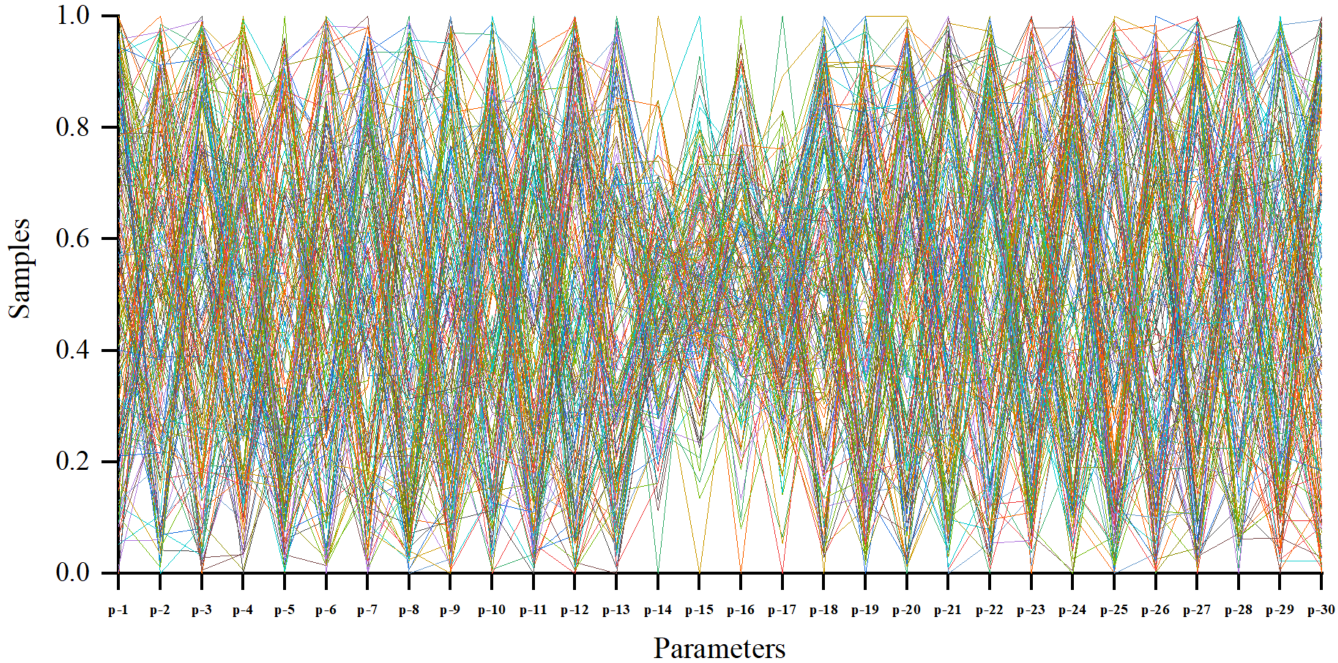

Fig. 5. Cobweb plot of the 181 random samples for the 30 parameters.

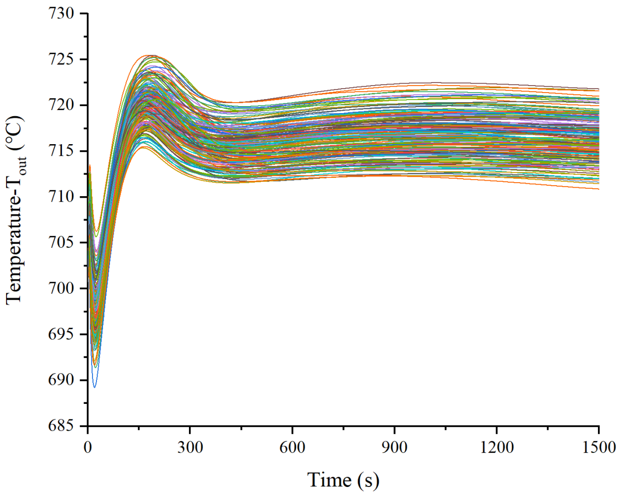

Fig. 6. Uncertainty propagation results of 181 cases for the reactor outlet fuel temperature(T_{out}).

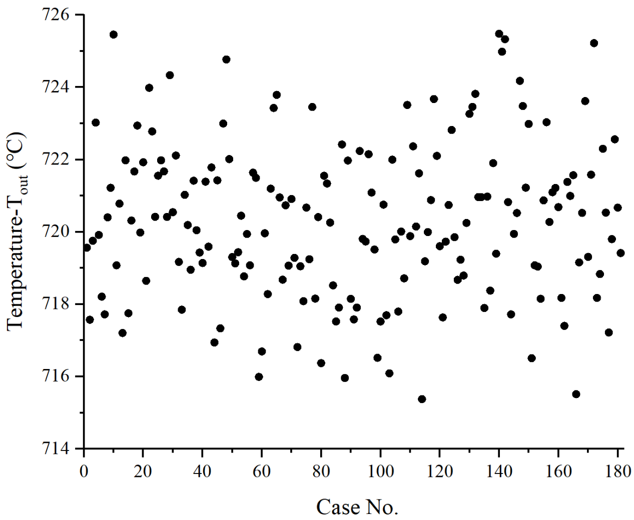

Fig. 7. Final value of T_{out_max} for 181 cases.

Based on above analysis, T_{out_max} follows a normally distributed. Table 4 shows the main statistical results and the T_{out_max} at different percentile according to the probability density function.

F. Sensitivity Analysis

In this paper, the multiple linear regression (MLR) method is adopted following the steps outlined in Fig. 3, to ascertain the importance of the input parameters. The F-test is used to assess whether the MLR models comply with statistical laws. The acceptance region is set to have an F-value greater than 1.83 at a significance level of 0.01. Table 5 lists the F value and R^2_{adj}. The results show that the model follow a quite convincing linear hypothesis relationship.

Fig. 11 shows the VIF values, all values are less than 5, therefore, SRCs of the input parameters were selected for sensitivity analysis. The absolute value of SRCs provide relative measure of the parameter importance and Fig. 12 shows the final absolute value of SRCs of 30 input parameters.

Furthermore, t-test is used to test the significance of sen-

Table 4. Statistical results of T_{out_max}.

variable	Mean	Standard deviation	Minimum	Maximum	Percentile(%)				
					95	96	97	98	99
Value (°C)	720.3	2.2	715.4	725.5	724.0	724.3	724.9	725.3	725.5

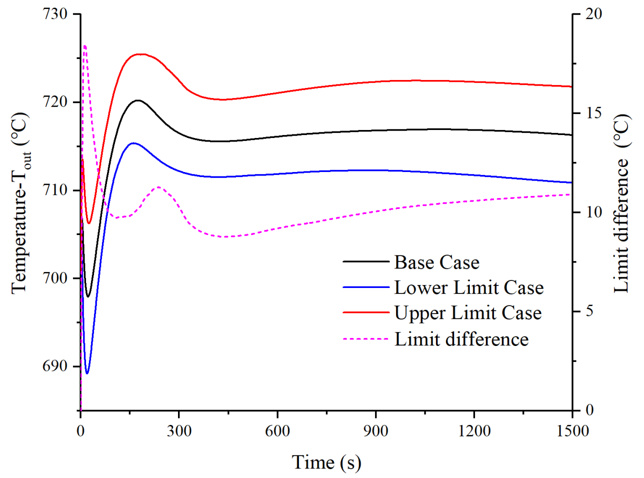

Fig. 8. Uncertainty analysis bound results for the reactor outlet fuel temperature (T_{out}).

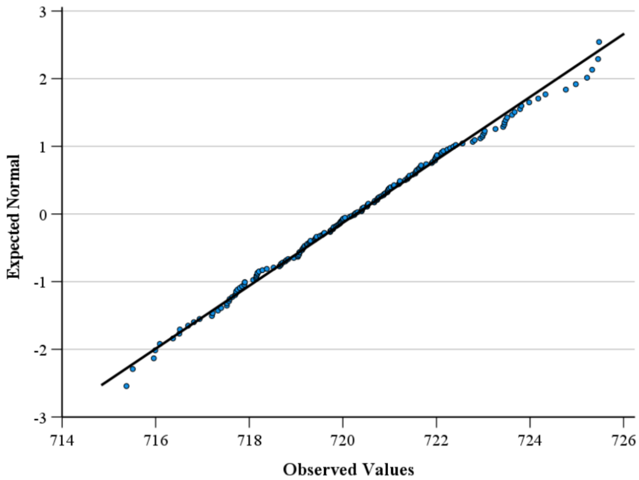

Fig. 10. Q-Q plot for T_{out_max}.

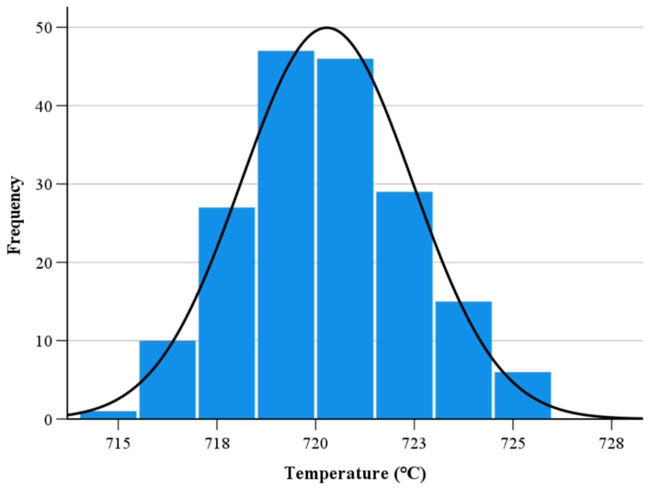

Fig. 9. Histogram and probability density function obtained from 181 simulations for T_{out_max}.

sitivity coefficient. The acceptable range is supposed to be the absolute value of t-value larger than 1.66 with a significance level of 0.05. Finally, five important parameters which are considered having a great contribution to LOFC consequences based on t-test and SRCs, are list in Table 6.

Unlike the traditional pressurized water reactors, which utilize solid fuels with fission energy transferred from the fuel pellet to cladding and finally to the coolant, SM-MSR uses liquid fuel salt which also serves as the coolant. In this system, fission energy is directly transferred to the coolant. Therefore, the reactor power, fuel salt flow in reactor, and properties of the fuel salt are very important to the LOFC consequences. Sensitivity analysis reveals that the Volume specific heat of the fuel salt (Density×specific heat) stands out as the most critical input uncertainty parameter, it affects heat absorption of fuel salt and the flow of fuel salt in the reactor core. Reactor power and reactor shutdown margin values can influence the heat generation after a scram, thus they will significantly impact the fuel salt temperature. The local resistance coefficients of the reactor core and the primary circuit play a crucial role in affecting fuel salt flow, making them important to the fuel salt temperature. Table 6 also shows the relationship between the 5 important input parameters and T_{out_max}. If SRC has a negative value, this indicates a negative correlation relationship, while a positive value signifies a positive correlation relationship.

Table 5. Statistical analysis results.

Parameter	F	R^2_{adj}
Value	887.9	0.993

G. Parameter Prediction

Multiple linear regression can used to predict the value of one variable by using the available information. Through the multiple linear regression method, confident predictive values of T_{out_max} can be obtained without a large number of calculations. This paper conducted a simple study on the prediction of T_{out_max} with the 5 important parameters.

The Weights of the parameters used for the prediction are

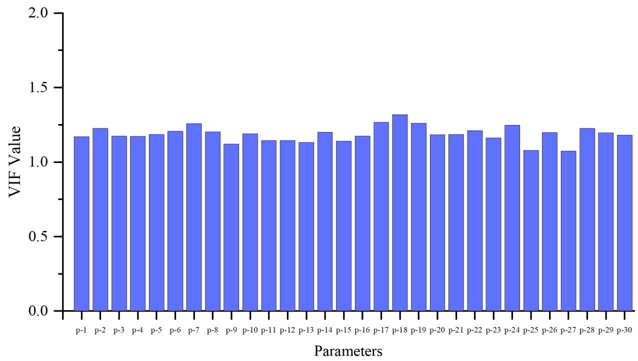

Fig. 11. VIF values of 30 parameters.

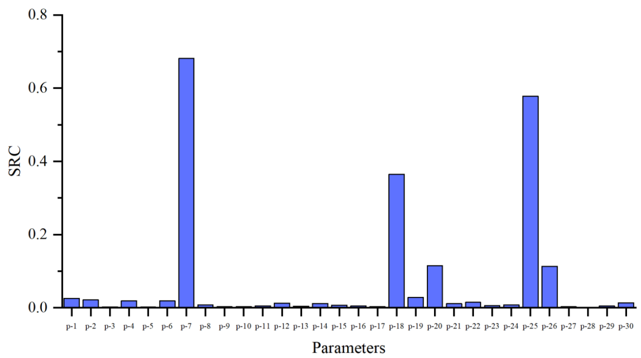

Fig. 12. Absolute value of SRCs final achieved.

Table 6. Most important parameters to LOFC consequences.

No.	Parameters		SRC	t
1	Volumetric heat capacity of fuel salt	Cpv_fuel	-0.681	-99.4
2	Local resistance coefficient of reactor core	f_core	0.578	91.1
3	Reactor power	P_reactor	0.365	52.0
4	Reactor shutdown margin	ρ_shutdown	-0.115	-17.3
5	Local resistance coefficient of primary circuit (excluding reactor core)	f_primary	0.113	16.9

shown in Table 7. RCSs of Cpv_fuel, and ρ_shutdown are negative, meaning there is a negative correlation relationship between those parameters and T_{out_max}, so the weights are arranged from large to small. Conversely, RCSs of P_reactor, f_core and f_primary are positive, so the weights are arranged from small to large, aiming to get conservative prediction of T_{out_max}.

It has been proven that T_{out_max} follow a normal distribution in chapter 4.4.2, and the significant statistic parameters used for prediction are listed in Table 4. Fig. 13 shows the predicted values of T_{out_max} and bounds of 95% prediction interval. The predicted upper bound value of the 11th case is 752.2 °C slightly exceeding 750 °C, and from Table 7, the weights are 0.6 or 1.4, uncertainty range is very large.

Table 7. Weights used for T_{out_max} prediction analysis

Case No.	Cpv_fuel	f_core	P_reactor	ρ_shutdown	f_primary
1	1.6	0.4	0.4	1.6	0.4
2	1.5	0.5	0.5	1.5	0.5
3	1.4	0.6	0.6	1.4	0.6
4	1.3	0.7	0.7	1.3	0.7
5	1.2	0.8	0.8	1.2	0.8
6	1.1	0.9	0.9	1.1	0.9
7	1.0	1.0	1.0	1.0	1.0
8	0.9	1.1	1.1	0.9	1.1
9	0.8	1.2	1.2	0.8	1.2
10	0.7	1.3	1.3	0.7	1.3
11	0.6	1.4	1.4	0.6	1.4
12	0.5	1.5	1.5	0.5	1.5
13	0.4	1.6	1.6	0.4	1.6

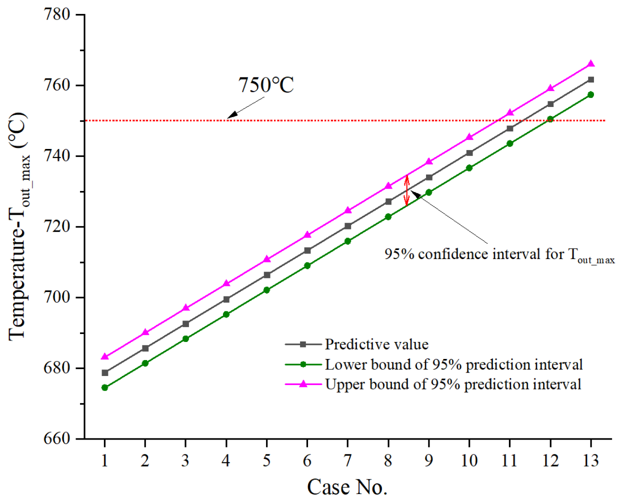

Fig. 13. Prediction of for T_{out_max} with the important 5 parameters.

V. CONCLUSIONS

In this paper, uncertainty and sensibility analysis of loss of forced cooling accident of a molten salt reactor were carried out based on Monte-Carlo and multiple linear regression method. An uncertainty analysis package for molten salt fluid system was developed and 181 samples of 30 input uncertainty parameters were propagated through RELAP5-TMSR, thus the uncertainty analysis package can be successfully executed. According to uncertainty analysis results, all the cases are lower than the acceptance criterion, and the maximum value of T_{out_max} is 725.5 °C, the minimum value of T_{out_max} is 715.4 °C. Additionally, identification of distribution was also performed in this study, and though statistical analysis, T_{out_max} is normally distributed.

According to statistical analysis, the multiple linear regression method can be used for molten salt reactor LOFC sensitivity analysis. Results show that Cpv_fuel, f_core, P_reactor, ρ_shutdown, f_primary are the most important parameters to LOFC consequences, and those parameters should be the key issues during the design and safety analysis of the 150MWt

SM-MSR.

After $\mathrm{T_{out\_max}}$ distribution was identified and sensitivity analysis was done, a simple study about the prediction of $\mathrm{T_{out\_max}}$ based on MLR method was implemented. When uncertainty of the five crucial parameters reached up to 40%, the predicted $\mathrm{T_{out\_max}}$ was $752.2\,^{\circ}\mathrm{C}$, and this value maintains a substantial safety margin compares with the acceptance criterion ($800\,^{\circ}\mathrm{C}$).

Subsequent research will be directed towards a comprehensive study of the uncertainty range of pivotal input parameters. And this will be achieved through a synergistic approach involving both experimentation and rigorous numerical analysis, with the ultimate aim of reducing the accident consequences uncertainty.

VI. BIBLIOGRAPHY

[1] M.H. Jiang, H.J. Xu, Z.M. Dai *et al*., Advanced Fission Energy Program - TMSR Nuclear Energy System, Bull. Chin. Acad. Sci. **27(3)**, p.366-374(2012). doi: 10.3969/j.issn.1000-3045.

[2] Z.M. Dai., Thorium molten salt reactor nuclear energy system (TMSR), in Molten salt reactors and thorium energy. ed. by T.J.Dolan (Woodhead Publishing, Cambridge, 2017), p.531–540.

[3] H.J. Xu, Z.M. Dai, X.Z. Cai, *et al*., Thorium based molten salt reactor and utilization of nuclear energy, Mod. Phys. **30(4)** p.25–34(2018).doi:10.13405/j.cnki.xdwz.2018.04.007.

[4] J.X. Zuo, C.M. Zhang., The Introduction of the Safety of Molten Salt Reactor. Nucl. Saf. **2011(3)**. doi: 10.3969/j.issn.1672-5360.2011.03.013.

[5] X.Z. Cai, Z.M. Dai, H.J. Xu, Thorium molten salt reactor nuclear energy system, Physics, **45(9)** p.578–590(2016).doi:10.7693/wl20160904.

[6] K. Wang, X.W. Jiao, Q. Yang *et al*., The effect of scram rod drop time on the consequences of molten salt reactor reactivity insertion transient, Nucl. Tech. **43(9)**, p.88-94(2020). doi: 10.11889/j.0253-3219.2020.hjs.43.090606.

[7] Q. Wei, L.W. Mei, Z.C. Zhan *et al*., Preliminary Study on Safety characteristics of Molten Salt Reactor, At. Energy Sci. Technol. **2014(12)**, p.2280-2286. doi: 0.7538/yzk.2014.48.12.2280.

[8] S.Z. Qiu, D.L. Zhang, W.X. Tai *et al*., Research on Inherent Safety and Relative Key Issues of a Moiten Salt Reactor. At. Energy Sci. Technol. **43(z1)**, p.64-75(2024).

[9] B. Zhou, X.H. Yu, Y. Zou *et al*., Study on dynamic characteristics of fission products in 2 MW molten salt reactor. Nucl. sci. Tech. **31(2)**. p.42-54(2020). doi: 10.1007/s41365-020-0730-z.

[10] L. Zhu, P. Pu, S. Du *et al*., Simulation of neutron diffusion and transient analysis of MSR. Nucl. Sci. Tech. **25(2)**. p.89-94(2014) doi:10.13538/j.1001-8042/nst.25.020601.

[11] W.X. Li, Q.N. Li, Molten Salt Reactor: A New Source of Innovation Development for Radiochemistry. J. Nucl. Radiochem., **38(06)** p.327-336(2016). doi: 10.7538/hhx.2016.38.06.0327.

[12] Y.P. Zhang, Y.W. Ma, J.H. Wu *et al*., Preliminary analysis of fuel cycle performance for a small modular heavy water-moderated thorium molten salt reactor. Nucl. Sci. Tech. **31(11)**, p.23-35(2020). doi: 10.1007/s41365-020-00823-5.

[13] Q. Wang, H.X. Yu, H.F. Zhang., Study on Molten Salt Circulation System in the Reactor of Nuclear Power Generation. Chem. Equip. Technol. **36(4)**, p.6-9,33(2015). doi: 10.3969/j.issn.1007-7251.2015.04.002.

[14] D.L. Zhang, S.Z. Qiu, C.L. Liu *et al*., Steady thermal hydraulic analysis for a molten salt reactor. Nucl. Sci. Tech. **19(3)**, p.187-192 (2008). doi: 10.1016/S1001-8042(08)60048-2.

[15] G.F. Zhu, W. Guo, X.Z. Kang *et al*., Neutronic effect of graphite dimensional change in a small modular molten salt reactor. Int. J. Energ. Res. **45(8)**, p.11976-11991 (2021). doi: 10.1002/er.5964

[16] F. D'Auria, Best estimate plus uncertainty (BEPU): status and perspectives. Nucl. Eng. Des. **352**, p.110190 (2019). doi: 10.1016/j.nucengdes.2019.110190

[17] X. Ran, X.H Zhang, J. Li *et al*., Overview in the Development of Best Estimate Plus Uncertainty Safety Analysis, Sci. Technol. Div. **24**, p.11-13,16 (2015). doi: 10.19694/j.cnki.issn2095-2457.2015.24.003

[18] X. Jiao, K. Wang, Y.H. Wu *et al*., Application of multiple linear regression to trip setpoint analysis in a reactivity initiated accident of a molten salt reactor. Int. J. Energ. Res. **45(8)**, p.11629-11641(2020). doi: 10.1002/er.5418.

[19] X.W. Jiao, K. Wang, C.Q. Wang *et al*., Study on sensitivity of initial conditions of reactivity initiated accident under low power conditions of molten salt reactor, Nucl. Tech. **44(6)**, p.82-88(2021). doi: 10.11889/j.0253-3219.2021.hjs.44.060602.

[20] M. Santanoceto, M. Tiberga, Z. Perkó, *et al*., Preliminary uncertainty and sensitivity analysis of the Molten Salt Fast Reactor steady-state using a Polynomial Chaos Expansion method. Ann. Nucl. Energy. **159**, p.108311 (2021). doi: 10.1016/j.anucene.2021.108311.

[21] J.J. Wang, Y. Dai, Y. Zou *et al*., Uncertainty analysis of heat transfer of TMSR-SF0 simulator. Nucl. Eng. Des. **56(2)**, p.762-769 (2024). doi: 10.1016/j.net.2023.11.016.

[22] M. Perez, C.M. Allison, R.J. Wagner, *et al*., The Development of RELAP/SCDAPSIM/MOD4.0 for Advanced Fluid Systems Design Analysis. 23th International Conference on Nuclear Engineering (ICONE-23), Chiba, Japan, May 17th-21st, 2015. ISBN-13:9784888982566.

[23] M. Pourgol-Mohammad, Thermal-hydraulics system codes uncertainty assessment: a review of the methodologies. Ann. Nncl. Energy. **36(11-12)**, p.1774-1786 (2009). doi: 10.1016/j.anucene.2009.08.018.

[24] M.P. Ferragut, Integration of a Quantitative-based Selection Procedure in an Uncertainty Analysis Methodology for NPP Safety Analysis. Universitat Politecnica de Catalunya. 2011.

[25] M. Khatib-Rahbar, E. Cazzoli, M. Lee *et al*., A Probabilistic Approach to Quantifying Uncertainties in the Progression of Severe Accidents. Nucl. Sci. Eng. **102(3)**, p.219-259(1987). doi: 10.13182/NSE89-A27476

[26] J. Baccou, J. Zhang, P. Fillion *et al*., Development of good practice guidance for quantification of thermal-hydraulic code model input uncertainty. Nucl. Eng. Des. **354**, p.110173(2019). doi: 10.1016/j.nucengdes.2019.110173

[27] K. Wang, X.W. Jiao, C.X. Cai, *et al*., Model validation for

the thermal hydraulic behavior in molten salt natural circulation. Proceedings of the 2018 International Congress on Advances in Nuclear Power Plants (ICAPP-2018), Charlotte, NC, United states, April 8th-11st, 2018. P.1199-1204. ISBN-13: 9780894487552

[28] S.S. Wilks, Determination of sample sizes for setting tolerance limits. Ann. Math. Stat. **12(1)** P.91-96(1941).

[29] S. Kang, J. Heo, C.W. Choi, *et al.*, Assessment study about the risk of Wilks' formula for uncertainty quantification of design extension condition scenarios in prototype Gen-IV sodium fast reactor. J. Nucl. Sci. Technol. **55(7)** P.746-755(2018). doi: 10.1080/00223131.2018.1435317.

[30] Y.S. Chen. Experimental and Simulation Research on Heat Transfer Characteristic of High Temperature Molten Salt and Molten Salt Heat Exchanger. University of Chinese Academy of Sciences, 2021

[31] R Jian, B Xu, MH Li, *et al.*, A specialized code for operation transient analysis and its application in fluoride salt-cooled high-temperature reactors. Nucl. Sci. Tech. **28(8)**, p.132-144(2017). doi: 10.1007/s41365-017-0268-x.

[32] T.Z. Zhou, K.C. Yu, M.S. Cheng *et al.*, Development and analysis of a K-nearest-neighbor-based transient identification model for molten salt reactor systems, Nucl. Tech. **46(11)**, p.122-132(2023) doi: 10.11889/j.0253-3219.2023.hjs.46.110604.

[33] Y.S. Song, M.S. Cheng, M. LIN *et al.*, Development and application of multi-scale thermal fluid coupling program for molten salt cooled fast reactor based on RELAP5 and sub-channel program, Nucl. Tech. **45(7)**, p.88-98(2022) doi: 10.11889/j.0253-3219.2022.hjs.45.070602.

[34] J.C. Helton, J.D. Johnson, C.J. Sallaberry, *et al.*, Survey of sampling-based methods for uncertainty and sensitivity analysis. Reliab. Eng. Syst. Safe. **91(10-11)**, P.1175-1209(2006). doi: 10.1016/j.ress.2005.11.017.

[35] Y. Kobayashi, S. Kondo, Y. Togo, Regression Model for Nuclear Characteristics of Sodium-Cooled Fast Reactor Core. J. Nucl. Sci. Technol. **12(1)**, P.61-63(1975). doi: 10.1080/18811248.1975.9733069.

[36] M. Feindt, M. Prim,An algorithm for quantifying dependence in multivariate data sets. Nucl. Instrum. Methods Phys. Res., Sect. A. **698**, P.84-89(2013). doi: 10.1016/j.nima.2012.09.043.

[37] G. Manache, C.S. Melching, Identification of reliable regression- and correlation-based sensitivity measures for importance ranking of water-quality model parameters. Environ. Modell. Softw. **23(5)**, P.1364-8152(2008). doi: org/10.1016/j.envsoft.2007.08.001.

[38] X.W. Jiao, S. Shao, K. Wang, *et al.*, Functional reliability analysis of a molten salt natural circulation system. Nucl. Eng. Des. **332**, P.127-136(2018). doi: 10.1016/j.nucengdes.2018.03.024.

[39] H. Glaeser, GRS Method for Uncertainty and Sensitivity Evaluation of Code Results and Applications. Sci. Technol. Nucl. Ins. **2008**, p.1-7, 26 Mar 2008. doi: 10.1155/2008/798901.

[40] T.G. Xu, Y. Zou, B. Xu *et al.*, ATWS accident analysis of rod withdrawal in small modular molten salt reactor. Nucl. Tech. **45(5)**, p.85-96(2022). doi: 10.11889/j.0253-3219.2022.hjs.45.050603.

[41] S.S. Shapiro, M.B. Wilk, An analysis of variance test for normality (complete samples). Biometrika. **52(3-4)**, p591-611(1965). doi: 10.1093/biomet/52.3-4.591.

[42] S.S. Dhar, B. Chakraborty, P. Chaudhuri, Comparison of multivariate distributions using quantile-quantile plots and related tests. Bernoulli. **20(3)**, p.1484-1506(2014). doi: 10.3150/13-BEJ530.